

Core-collapse supernovae: from “nu” physics to new physics

Meriem Bendahman,^{a,e,*} Paul Barrère,^b Anne-Cécile Buellet,^b Matteo Bugli,^{b,c} Joao A. B. Coelho,^a Alexis Coleiro,^a Gwenhaël de Wasseige,^d Sonia El Hedri,^a Thierry Foglizzo,^b Davide Franco,^a Isabel Goos,^a Jérôme Guilet,^b Antoine Kouchner,^a Raphaël Raynaud^b and Yahya Tayalati^{e,f}

^a*Université Paris Cité, CNRS, Astroparticule et Cosmologie
10 rue Alice Domon et Léonie Duquet, Paris, France*

^b*Université Paris-Saclay, Université Paris Cité, CEA, CNRS, AIM
Gif sur Yvette, France*

^c*Dipartimento di Fisica, Università di Torino
Via P. Giuria 1, Torino, Italy*

^d*Université Catholique de Louvain
Pl. de l'Université 1, Louvain la Neuve, Belgium*

^e*Faculty of Sciences, Mohammed V University
Avenue des Nations Unies, Rabat, Morocco*

^f*Institute of Applied Physics, Mohammed VI Polytechnic University
Ben Guerir, Morocco*

E-mail: mbendahman@km3net.de

Core-collapse supernovae (CCSNe) are important astronomical events that provide crucial information about the dynamics of galaxies. The time profile of neutrinos in core-collapse supernovae is a unique and valuable source of information about the mechanism of collapsing stars and the behavior of particles in highly dense environments. However, as close-by supernovae are rare, only one observation of supernova neutrinos has been made to date. To make the most of the next galactic CCSN, observations from multiple neutrino experiments need to be combined in real-time, and the results quickly transmitted to optical telescopes. Locating the CCSN will notably be a major challenge and requires disentangling localization information from signatures associated with the supernova progenitor properties or the physics of the neutrinos themselves. Consequently, existing CCSN distance measurement algorithms need to assume that neutrino properties are well-predicted by the Standard Model. In this contribution we present an approach to extract and separate information about the CCSN and the physics of the neutrinos in a fast and simple way. We show how this approach can be made robust against the new physics effects most susceptible to bias CCSN measurements, by taking advantage of the diverse landscape of next-generation neutrino detectors.

38th International Cosmic Ray Conference (ICRC2023)
26 July - 3 August, 2023
Nagoya, Japan



*Speaker

1. Introduction

Core-collapse supernovae (CCSNe) provide crucial insights into the dynamics of galaxies. If a CCSN occurs in the Milky Way, the neutrino burst emitted by its core could be detected before the explosion becomes visible. Due to the rarity of galactic supernovae, reliable CCSN localization information should be extracted from neutrino data and sent to telescopes as quickly as possible. In particular, knowing the CCSN distance, could allow determining whether the supernova occurred in the dust-obscured regions behind the galactic center, thus affecting observation strategies [1]. However, disentangling the effect of this distance from the ones of the progenitor and neutrino properties on observations is extremely challenging. Current CCSN distance measurement strategies mitigate the dependence in the progenitor but assume standard neutrino flavor conversion mechanisms [2, 3]. Approaches to constrain neutrino properties typically rely on energy measurements [4], which are not available at all experiments. Within the next 20 years, however, the palette of neutrino detectors sensitive to CCSNe will change drastically: water Cherenkov detectors will be joined by experiments sensitive to other combinations of neutrino flavors. This *flavor-complementarity* could allow lifting the degeneracies between neutrino and CCSN properties before event reconstruction, thus accelerating the data transmission to the Supernova Early Warning System (SNEWS) [5].

In this contribution, we propose an algorithm to simultaneously constrain the CCSN position, the progenitor characteristics, and neutrino properties, using only neutrino counting rates measured at large-scale next-generation experiments. We assess this algorithm’s capability to locate CCSNe and characterize neutrinos with minimal information and we evaluate its robustness in the presence of non-standard interactions such as neutrinos two-body decays.

2. Methodology

To investigate the imprints of CCSN and neutrino properties on observations, we evaluate the expected neutrino rates for a selection of current and upcoming experiments, a comprehensive set of supernova models, and different flavor conversion mechanisms. This section describes this procedure as well as the observables we will use for CCSN characterization.

CCSN models: This analysis considers a set of 149 progenitor models designed and introduced by Sukhbold *et al* in [6]. These models, based on one-dimensional simulations, cover the wide range of progenitor parameters (e.g. masses, compactness, metallicity) expected for CCSNe with an iron core and were designed in order to identify observables with a weak dependence in the CCSN model, hence being ideally suited to our study. We define these models’ probability distribution w using the Salpeter Initial Mass Function: $w(M) \propto M^{-2.35}$ with M the progenitor mass.

Neutrino experiments Next-generation large-scale detectors will be sensitive to three neutrino flavor combinations: electron antineutrinos for water Cherenkov (WC) detectors, electron neutrinos for kiloton-scale liquid argon detectors, and the sum of all neutrino flavors for experiments sensitive to Coherent Neutrino-Nucleus scattering (CE ν NS). For WC detectors, we consider Hyper-Kamiokande (HK), IceCube, and KM3NeT. For large liquid argon experiments, we choose DUNE’s far detector, the largest project to date. Finally, for CE ν NS detection experiments, we consider DarkSide-20k as well as a similar, but 7 times bigger, project called ARGO.

Neutrino flavor conversion models This analysis will focus on the first 150 ms of the CCSN, where flavor-conversion mechanisms inside the star are dominated by adiabatic MSW flavor transitions. Due to the MSW effect, the flavor composition of neutrinos reaching Earth will strongly depend on the mass ordering. Additionally, we study scenarios where neutrinos undergo two-body decays. Indeed, these Beyond the Standard Model (BSM) interactions are among the few proposed classes of new physics phenomena which could both mimic SM scenarios and lead to biased distance and mass ordering estimates [7]. Here, we take the example of the Dirac ϕ_0 scenario from [7], where the heaviest neutrino species decays into the lightest. We thus introduce 2 parameters: the ratio \bar{r} of the CCSN distance over the decay length, and the branching ratio ζ to active neutrinos.

Analysis pipeline We evaluate expected neutrino rates at the different detectors using the SNEWPY software [8]. We modified SNEWPY to incorporate the neutrino decay model described above, as well as detection efficiency curves for DarkSide-20k and ARGO [9]. For IceCube and KM3NeT, Poissonian backgrounds are added, with rates of 1.5 MHz and 3 MHz, respectively.

Building block observables This analysis is based on observables with a low or easily parametrizable dependency in the CCSN model. Most of these observables have already been proposed in the literature [2, 3] as “standard candles” for CCSN distance measurements at single detectors. First, we consider the expected numbers of signal events in the first 10, 20, 30, 40, and 50 ms after the CCSN detection. As shown in figure 1, these numbers depend only weakly on the CCSN progenitor properties. While earlier time windows exhibit a weaker CCSN model dependence, the reduced statistical uncertainties for larger windows might lead to more precise measurements. Second, we consider ratios between the rates described above and the rates measured in the early accretion phase, 100 to 150 ms after the beginning of the CCSN. This choice is based on [2], which demonstrated that using these ratios could mitigate the residual model-dependence of early neutrino rates for CCSN distance measurements. The associated observables, called f_Δ and shown in figure 1, depend quasi-linearly on the early neutrino rates:

$$f_\Delta(\Delta t) = \frac{N(100 - 150 \text{ ms})}{N(\Delta t)} \approx \alpha N(\Delta t) + \beta \quad (1)$$

In [2], Δt was taken to be 50 ms; here we consider 10 to 50 ms windows, as described above.

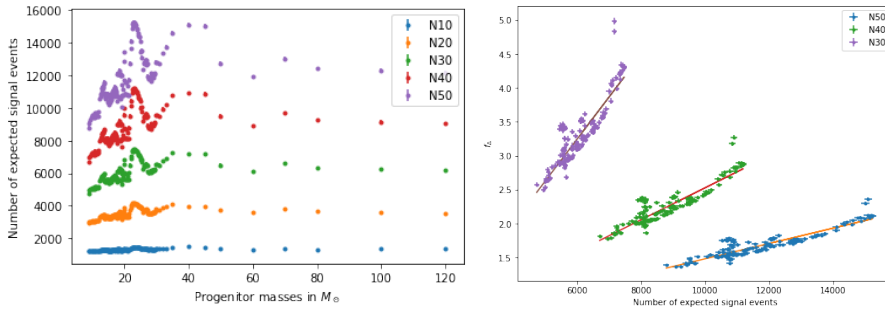


Figure 1: Left: CCSN neutrino rates for IceCube detector for IMO as a function of progenitor masses. Each color represent a time window, from blue to violet, going from the first 10 ms to the first 50 ms. Right: f_Δ fitted as a function of CCSN rates considering 3 time windows: 30 ms, 40 ms and 50 ms.

3. Constraining neutrino properties with stable observables

This section presents a simple study aimed at estimating the capability of different observables and detector combinations to probe neutrino properties, focusing on the determination of the neutrino mass ordering (MO). We use the observables introduced in section 2 to build two sets of variables which depend only weakly on the CCSN model and position: the ratios between early-time neutrino rates (subtracting the expected background rates) at two different detectors i and j $\mathcal{R}_{ij} = N_i(\Delta t)/N_j(\Delta t)$, and the ratios $\mathcal{F}_{ij} = \alpha_i/\alpha_j$ where α_{ij} is obtained from equation 1 by computing $f_{\Delta,ij}$ from data and taking β_{ij} from simulations. By construction, the central values of these variables do not depend on the CCSN distance.

Assuming the CCSN distance is known, we evaluate the capability of each single observable to discriminate between the normal (NMO) and inverted (IMO) mass orderings. To this end, for a detector pair ij , and a true model M , we compute the probability $\mathcal{P}_{ijM}(M')$ for a “typical” NMO (IMO) measurement—with observed rates equal to their expectation values—to be observed under the IMO (NMO) hypothesis for a CCSN model M' . The p-value is then given by $p = \sum_{M' \in \text{models}} \mathcal{P}_{ijM}(M') w(M')$ with $w(M')$ defined in section 2.

The maximal CCSN distances at which the IMO (NMO) can be rejected by more than 3σ (or 3σ distance horizons) are shown on the left (right) panel of figure 3 for all possible \mathcal{R} and \mathcal{F} observables and detector pairs. Overall, pairs of flavor-complementary experiments perform significantly better than other pairs, with distance horizons extending far beyond the galactic center. Finally, in most cases, observables involving rates observed in the first 10, 20, and 50 ms of the CCSN perform best and including the 100 – 150 ms region sizably reduces model-related uncertainties.

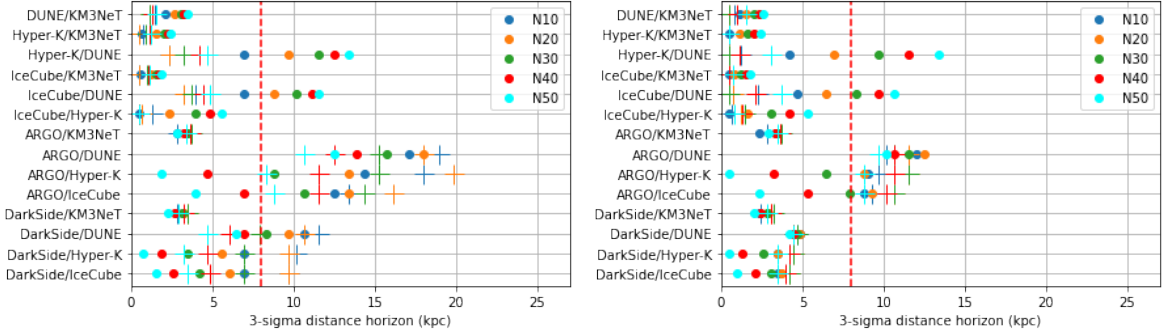


Figure 2: 3σ distance horizon for rejecting the IMO (left) and the NMO (right), for a $9M_{\odot}$ CCSN progenitor. The dots and crosses represent the \mathcal{R} and \mathcal{F} observables, respectively. The colors refer to the size of the time window. The red dashed line corresponds to the galactic center.

4. CONSTRAIN CCSN PROPERTIES

We now present an analysis strategy to simultaneously constrain the CCSN position in the sky, its progenitor properties, and neutrino flavor conversion parameters, using multiple detectors. The simple study presented in section 3 showed that neutrino rates observed within the first 10, 20, and 50 ms of the CCSN were the most sensitive to the neutrino MO, and that considering the 100 – 150 ms period could considerably reduce the dependence in the CCSN model. We therefore

build a likelihood function with four time bins for each detector: 0 – 10 ms, 10 – 20 ms, 20 – 50 ms, and 100 – 150 ms, with the zero being the supernova detection time. For a given set of observations $\{O_{\text{obs}}\}$, this likelihood can be written as

$$\log \mathcal{L}(\{O_{\text{obs}}\}|d, M, \bar{r}, \zeta, \text{ordering}) = \log w(M) + \sum_i P[N_i(10\text{ms})] + P[N_i(10 - 20\text{ms})] + P[N_i(20 - 50\text{ms})] + P[N_i(100 - 150\text{ms})] \quad (2)$$

where i is the detector index, d the CCSN distance, and (\bar{r}, ζ) are the neutrino decay parameters defined in section 2. The CCSN model is given by the parameter M with probability $w(M)$ proportional to the Salpeter IMF. P is the Poisson probability for observing a given number of events; its expectation value will depend on d, M, \bar{r}, ζ and the MO. In what follows, we will consider either the *SM-only* assumption, $\bar{r} = 0$, or the *BSM* assumption, where \bar{r} and ζ can vary.

4.1 Breaking degeneracies: neutrino mass ordering

We use the likelihood defined in equation 2 to determine the neutrino MO, this time without knowing the CCSN distance. We first assume that neutrino properties are described by the SM and, for a given measurement, we maximize the likelihood over the supernova model and distance for each MO hypothesis. We then compute the p-value of a typical IMO or NMO measurement, taking the ratio between the IMO and NMO likelihoods as our test statistics. The left panel of figure 3 shows the 3σ distance horizon for rejecting the IMO with a typical NMO measurement, for single detectors and pairs of experiments. For DUNE, HK, IceCube, and ARGO, pairing complementary detectors significantly increases the distance horizon, sometimes beyond the edge of the Milky Way. To assess the robustness of this result in the presence of strong rate distortions from new physics effects, we repeated this procedure for a model with $\bar{r} = 5$ and $\zeta = 1$. This time, under the SM-only hypothesis, all discriminating power is lost, as expected from [7]. However, when optimizing the likelihood over \bar{r} and ζ , distance horizons can extend up to 22 kpc for detector pairs, as shown in figure 3. Here, pairing detectors is essential to discriminate between models, especially for DUNE.

4.2 Measuring supernova distances

We now use the likelihood from equation 2 to assess how new physics could bias CCSN distance measurements, and whether these biases could be reduced by combining experiments. To this end, we evaluate CCSN distances by optimizing the likelihood over the supernova model, as well as \bar{r} and ζ for the BSM assumption, assuming the mass ordering is known. Figure 4 shows the 90% confidence intervals on the measured distance for a $9M_{\odot}$ CCSN at 10 kpc, in the SM, with the SM-only assumption. In the IMO, combining flavor-complementary detectors can reduce distance uncertainties by almost a factor of 2, even when adding a new experiment does not sizeably increase the statistics. Conversely, as shown in figure 5 for $\bar{r} = 5$ and $\zeta = 1$, neutrino decays could significantly bias distance measurements in experiments like DUNE or ARGO. Optimizing the likelihood on (\bar{r}, ζ) removes this bias but considerably increases uncertainties for individual experiments. However, when combining two detectors, these uncertainties decrease more than threefold, reaching 6% at 10 kpc in the IMO for a DUNE+HK combination. Our approach could therefore allow alert systems to disentangle neutrino properties from CCSN localization information,

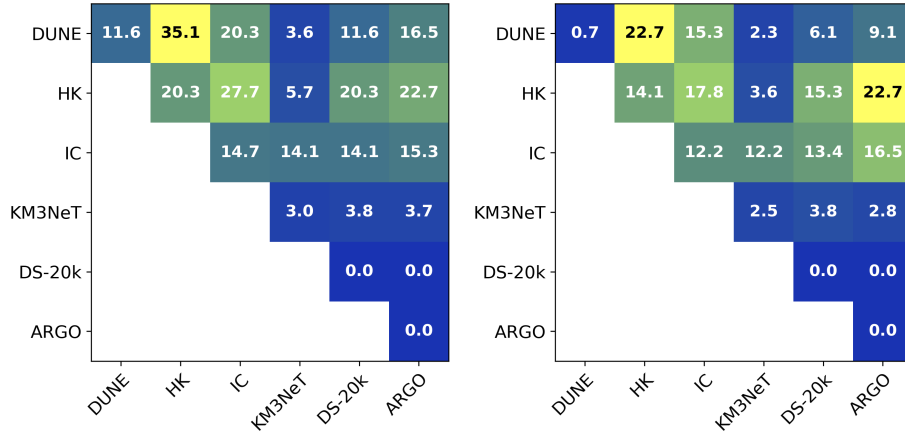


Figure 3: Distance horizons (in kpc) for a 3σ rejection of the IMO with a “typical” NMO measurement where the observed rates are equal to their expectation values. Left: SM scenario with SM likelihood. Right: BSM scenario with $\bar{r} = 5$, $\zeta = 1$ and BSM likelihood. Diagonal terms correspond to single detectors. Since DarkSide-20k and ARGO treat all neutrino flavors equally they are not sensitive to the mass ordering.

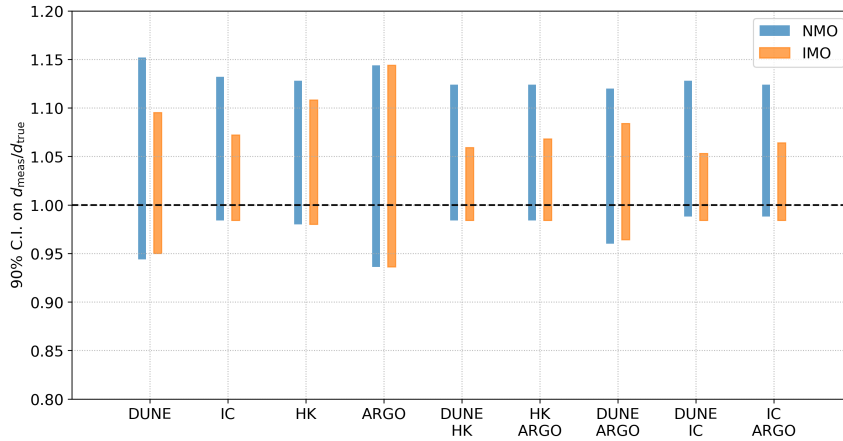


Figure 4: 90% confidence intervals on the measured CCSN distance for a $9M_{\odot}$ progenitor at 10 kpc, in the SM, with the SM-only assumption, for different experiments (singles or pairs).

even without energy reconstruction. Moreover, the method proposed here is fast: with a simple Jupyter notebook on a personal computer, the 90% confidence band evaluation takes about 5 s in the SM-only case and between 15 s (single detector) and 30 s (pair) when optimizing \bar{r} and ζ .

4.3 Identifying deviations from the SM

As discussed above, new physics phenomena in the neutrino sector could bias CCSN localization. Here, we evaluate the compatibility of a CCSN observation with the SM by comparing the best-fit likelihood of an observation to the likelihood distribution for all possible SM observations. We estimate this SM distribution using 10^5 pseudo-experiments and assume that the mass ordering is known. Figure 6 shows how combining DUNE with complementary experiments affects the 3σ distance horizon for a SM rejection. While 3σ deviations from the SM could be identified up to

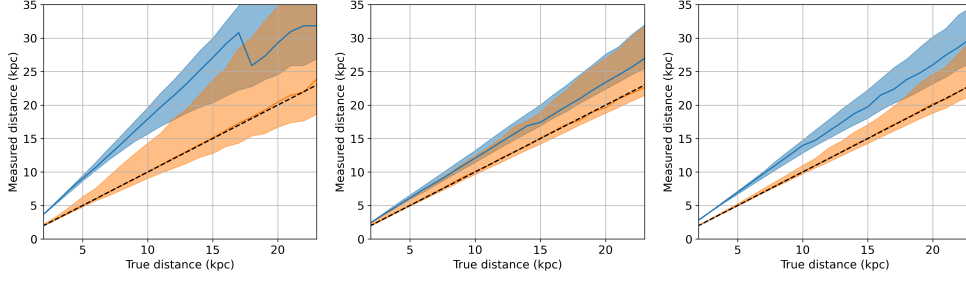


Figure 5: Best-fit distance and 90% C.I. for DUNE (left), HK (middle), and DUNE+HK (right), for a $9M_{\odot}$ CCSN with $\bar{r} = 5$, $\zeta = 1$, in the IMO. The SM-only assumption is shown in blue and the BSM assumption in orange. The jagged line for DUNE stems from numerical issues due to near-degeneracies between models.

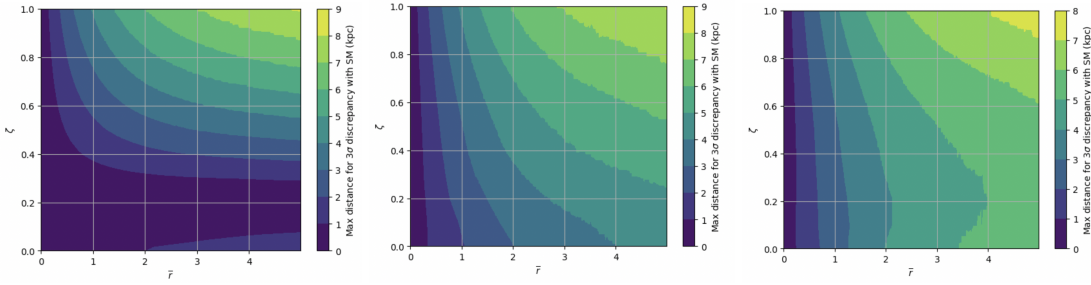


Figure 6: 3σ distance horizon for rejecting the SM, for a $9M_{\odot}$ progenitor, in the NMO, for measurements performed at DUNE, DUNE+ARGO, and DUNE+HK+ARGO.

9 kpc at DUNE alone for large ζ , results are almost degenerate with the SM at low ζ . Combining DUNE with ARGO lifts this degeneracy and further improvement can be obtained for $\zeta < 0.2$ by adding HK, at the price of a mild decrease in reach for high ζ . While these 3σ distance horizons reach only a few kiloparsecs, alert systems could consider different p-value thresholds with different responses (fits with BSM assumptions, visual inspection, etc...). Expected p-values for individual experiments could also be computed by realtime analysis systems and included in alert bulletins.

4.3.1 Fitting neutrino decay parameters

In this contribution, we have shown how to combine complementary detectors to reduce the impact of BSM neutrino properties on CCSN localization and mass ordering measurements. We now show that the likelihood from equation 2 can be used to characterize neutrino decay models. To this end, we optimize this likelihood over the pre-supernova model and the CCSN distance, and consider its variations as a function of (\bar{r}, ζ) . We consider a $9M_{\odot}$ progenitor at 10 kpc and typical observations, corresponding to the expectation values for the models considered. Figure 7 shows iso-likelihood contours for the NMO and for a decay model with $\bar{r} = 2$, $\zeta = 0.5$, for different experiments. For DUNE alone, we again see the degeneracy region mentioned in the previous section. Again, this degeneracy is lifted by combining DUNE with ARGO and a visible improvement can be seen when adding HK. Hence, using a minimal amount of information and simple observables, the approach proposed in this contribution could allow setting meaningful constraints in unexplored regions of the parameter space for BSM neutrino models.

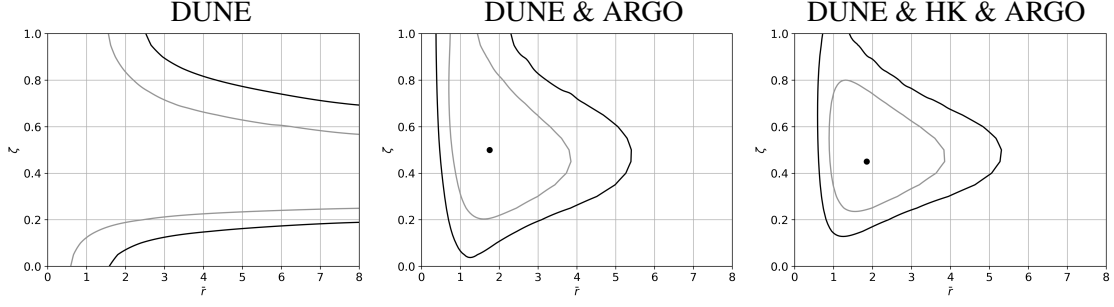


Figure 7: Best-fit value (black dot), and contours for $-2 \log \mathcal{L}_{\max}$ plus 2.3 (grey) and 4.6 (black) where \mathcal{L}_{\max} is the maximum likelihood, in the (\bar{r}, ζ) space for a $9M_{\odot}$ progenitor at 10 kpc, in the NMO with $\bar{r} = 2$, $\zeta = 0.5$. Results are shown for DUNE (left), DUNE+ARGO (middle), and DUNE+ARGO+HK (right).

5. Conclusion

In this contribution, we presented a method to simultaneously extract information about the CCSN location, the progenitor properties, and the physics of neutrinos, with minimal information about the neutrino rate. With this approach, 3σ sensitivity on the neutrino mass ordering can be obtained for the entire galaxy. We demonstrated the vulnerability of current CCSN localization techniques to new physics effects. We showed that this vulnerability can be overcome by combining complementary experiments, taking advantage of the fact that neutrino decays are among the leading proposed BSM scenarios which could impact early-time CCSN rates. The strategy proposed here could provide a way for alert systems to make the most of the rich landscape of next-generation neutrino experiments.

6. Acknowledgements

This work is supported by LabEx UnivEarthS (ANR-10-LABX-0023 and ANR-18-IDEX-0001). We thank Maria Cristina Volpe and Joachim Kopp for interesting and helpful discussions.

References

- [1] K. Nakamura *et al.*, Mon. Not. Roy. Astron. Soc. **461** (2016) no.3, 3296-3313.
- [2] M. Segerlund *et al.*, arXiv:2101.10624v1 [astro-ph.HE].
- [3] M. Kachelriess *et al.*, Phys. Rev. D 71 (2005) 063003.
- [4] X.-R. Huang *et al.*, arXiv:2305.00392 [hep-ph].
- [5] SNEWS Collaboration, New J. Phys. 23 (2021).
- [6] T. Sukhbold, *et al.*, Astrophys. J. 821, 38 (2016).
- [7] A. de Gouvea *et al.*, Phys. Rev. D 101 (2020) 4, 043013.
- [8] A. Baxter *et al.*, J. Open Source Softw. **6** (2021) no. 67, 3772.
- [9] DarkSide Collaboration, JCAP 03 (2021) 043.